Colloid Polym Sci (2007) 285:449–455
DOI 10.1007/s00396-006-1586-4

ORIGINAL CONTRIBUTION

# Melting behavior of lamellae of isotactic polypropylene studied using hot-stage atomic force microscopy

**Xi Wang · Weimin Hou · Jianjun Zhou · Lin Li · Yang Li · Chi-Ming Chan**

Received: 13 April 2006 / Accepted: 11 September 2006 / Published online: 4 November 2006


**Abstract** The α- and β-form lamellae of isotactic polypropylene were developed at different temperatures. The melting behaviors of the lamellae were observed in real time at elevated temperatures using a hot-stage atomic force microscopy. The melting behavior of the α-form lamellae was determined by the lamellar defects. For the α-form lamellae developed at different undercoolings, the larger the undercoolings, the relatively higher amount of defect in the lamellae was observed. The lamellae with defects were melted into lamellar segments, and recrystallization took place during the heating process. The β-form lamellae had lower thermal stability, and they melted firstly and separately from that of α-form.

**Keywords** Isotactic polypropylene · Melting · Atomic force microscopy (AFM) · Lamellae

X. Wang · W. Hou · J. Zhou (✉) · L. Li
Beijing National Laboratory for Molecular Sciences (BNLMS), State Key Laboratory of Polymer Physics and Chemistry, Institute of Chemistry, Chinese Academy of Sciences, Beijing 100080, China
e-mail: pla_zjj@iccas.ac.cn

Y. Li
Department of Polymer Science and Materials, The School of Chemical Engineering, Dalian University of Technology, Dalian 116012, China

C.-M. Chan
Department of Chemical Engineering, Hong Kong University of Science and Technology, Clear Water Bay, Hong Kong, China

*Present address:*
X. Wang · W. Hou
Graduate School of the Chinese Academy of Sciences, Beijing, China

## Introduction

Isotactic polypropylene (*i*-PP) is a very important semi-crystalline polymer, and the crystallization and melting behaviors of *i*-PP samples have been well studied. Usually, multiple melting peaks can be observed during differential scanning calorimetry (DSC) measurements. However, the crystal polymorphs (such as α-, β-, γ-, and mesomorphic forms), crosshatched lamellae, molecular fractionation, and isotacticity complicate the interpretation of the multiple melting peaks. Among the factors that have ever been suggested to explain multiple melting peaks of *i*-PP are the different crystal structures [1, 2], different lamellar thickness [3], different crystal sizes [4–9], and melting and recrystallization of lamellae [10–15].

Whereas the multiple melting peaks are considered to originate from morphological or structural variations, it is commonly accepted that only two major crystal forms (α and β) are involved [4–9]. During crystallization, α spherulites are the most commonly found form, and the multiple peaks should arise mainly from α crystal regions alone, with a little influence of the β-form [16]. The multiple melting peaks of α-form crystals formed at high undercooling originated from the recrystallization and perfection during heating [10–15], whereas at low undercooling, two populations of crystals with different thermal metastabilities melted separately, leading to the multiple melting peaks [4–9]. Transmission electron microscope (TEM) studies have verified that radial dominant lamellae have a larger lamellar thickness than that of the tangential lamellae in spherulites formed at low undercooling [5, 17]. Mezghani et al. [3] found that during heating, the first effect observed is an increase in the birefringence of the spherulites, which in turn is attributed to the melting of tangential branches at a lower temperature than the dominant lamellae.

Although the α-form is the most common, the β-form spherulites can be formed under some special conditions such as orientation or deformation in the melt [18], the presence of large temperature gradients [19], or the introduction of special nucleating agents [20–22]. If the β-form is present, the phase transition from β to α can be easily observed with polarized optical microscopy (POM) and can be identified from DSC, and such studies lead to conclusion that the β-form has less thermodynamic stability than the α-form [19].

Morphological developments upon the melting of *i*-PP polymers have been extensively investigated using POM [1, 23, 24]. Recently, Weng et al. [8, 9] studied the melting morphology under TEM by partially melting a specimen between the two melting peaks and assigning the higher peak to radial dominant lamellae and the lower peak to tangential subsidiary lamellae, filling the space in between. They suggested that the development of these double endotherms was influenced by crosshatching and is related to morphological constraint rather than to molecular fractionation. But at the same time, they found that the materials, crystallized at 160 °C with no crosshatching present, still exhibit double endotherms. Using TEM, remarkable insights into the lamellar structures of semi-crystalline polymers have been obtained. However, this technique cannot be used to examine melting and crystallization in real time. Most recently, hot-stage atomic force microscopy (AFM) has been applied to image crystallization and melting of polymers in real time [25–27]. Winkel et al. [26] examined the annealing behavior of once-folded crystals of the long-chain alkane, $C_{162}H_{326}$, in real time using AFM. At the same time, Zhou et al. [27] performed in situ single crystal melting experiments on syndiotactic polypropylene. Very recently, we studied the melting behavior of the lamellar crystals of poly(bisphenol A-*co*-decane ether) prepared at different undercoolings in real time at elevated temperatures using AFM [28]. It is observed that for lamellae formed at high undercoolings, melting is accompanied by recrystallization, whereas for lamellae formed at low undercoolings, melting starts from the edges and proceeds to the center.

Previous morphological studies of *i*-PP melting behavior were restricted to inherently low-resolution optical microscopic measurements in real time or TEM discontinuous observation with high resolution. In this work, the melting behaviors of both α- and β-form lamellae were monitored in real time using a hot-stage AFM with high resolution.

## Experimental section

An *i*-PP with $\overline{M}_W = 4.12 \times 10^5$ and $\overline{M}_W/\overline{M}_N = 5.5$, as measured by gel permeation chromatography, was bought from Aldrich. It was dissolved in boiling *p*-xylene at 138 °C with a concentration of 10 mg $ml^{-1}$. Thin films with a thickness of around 200 nm were prepared by spin coating hot polymer solutions onto a freshly cleaved surface of mica, which was preheated to 80 °C before spin coating for the solvent to evaporate quickly. The films were then dried in a vacuum oven at 50 °C for 24 h to remove the solvent.

AFM tapping-mode images were acquired using an AFM (NanoScope IIIA MultiMode™ Digital Instrument) equipped with a high-temperature heater accessory. The experimental details of high-temperature AFM can be found elsewhere [27, 28]. Both height and phase images were recorded simultaneously, and only phase images were presented here. The setpoint amplitude ratio ($r_{sp} = A_{sp}/A_0$ where $A_{sp}$ is the setpoint amplitude and $A_0$ is the amplitude of the free oscillation) was adjusted to 0.7–0.9. Si tips (TESP, Digital Instruments) with a resonance frequency of approximately 300 kHz and a spring constant of about 40 N $m^{-1}$ were used. Before AFM observation, the *i*-PP thin film was isothermally crystallized at a specific temperature under $N_2$ protection after it was melted on the AFM hot stage at 200 °C for 4 min. Then, the melting process of the newly formed lamellae was observed by AFM in real time. For the growth of β-form lamellae, a selective β-nucleating agent was used to induce the growth of the β-form spherulites.

## Results and discussions

*Melting behaviors of α-form lamellae* The lamellar structures and thermal behaviors of α- and β-forms of *i*-PP have been reported in our previous papers [29, 30]. Edge-on crosshatched and flat-on lath-like lamellae of α-form and extended sheet-like flat-on lamellae of β-form can be easily identified by AFM phase imaging.

Figure 1 shows the melting and recrystallization process of edge-on lamellae of *i*-PP formed at 146 °C. Densely crosshatched structures consisted of tangential and radial lamellae can be observed, and the radial growth direction is indicated by an arrow, as shown in Fig. 1a. The angle between tangential and radial lamellae is about 80°, which has been known to be the result of homoepitaxial growth of tangential lamellae on the (010) plane of a parent radial lamella. Comparing Fig. 1a–d, it can be found that some of the infilling species melt first as the temperature increased, and the densely crosshatched structures gradually become sparse. Typical melting behavior of the lamellae is exemplified by the framed area A. As the temperature is increased from 146 to 163 °C, some of the infilling species disappear, and the densely crosshatched structures gradually become sparse, as shown in Fig. 1a–c. It can also be

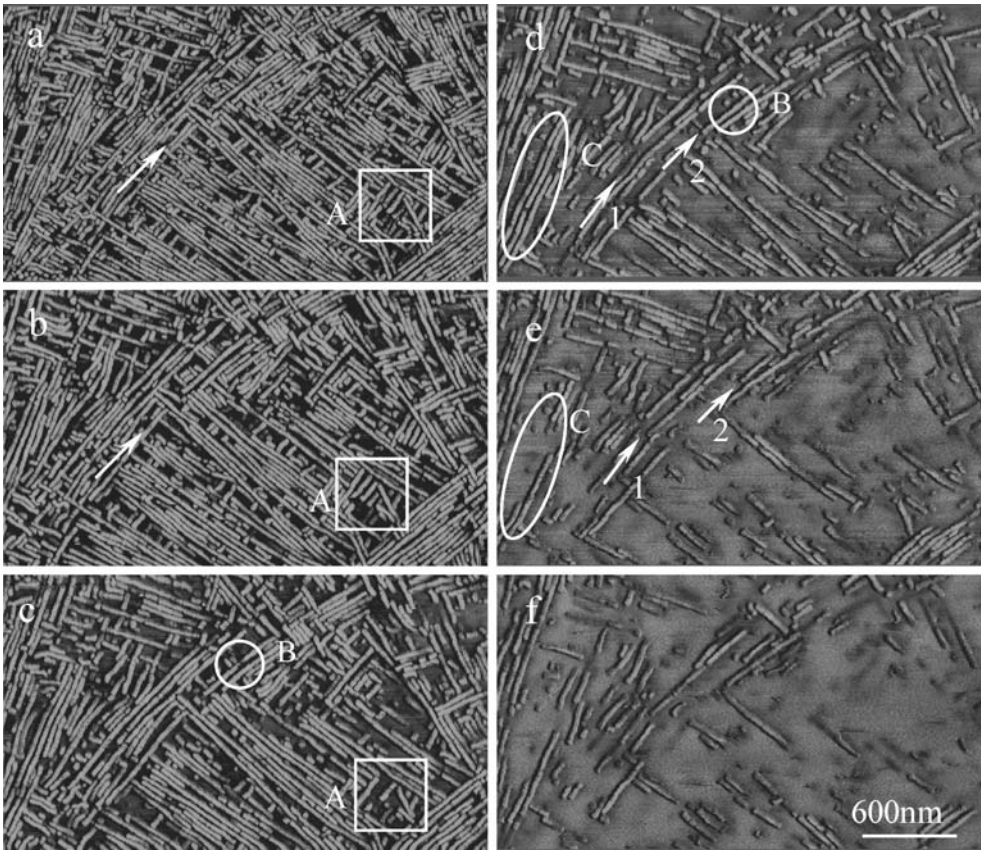


**Fig. 1** Melting of crosshatched lamellae formed at 146 °C for about 60 min; **a** 146 °C, **b** 163 °C, **c** 163 °C, **d** 165 °C, **e** 166 °C, and **f** 167 °C. The time interval between two consecutive images is about 30 min

found that different lamellae show different melting behaviors, and the melting process can be clearly observed from Fig. 1c–e. Some of the lamellae retract from one end, and some break into segments, as shown by arrows 1 and 2 and circle C in Fig. 1d and e. Recrystallization or reorganization can also take place at the same temperature of melting, as shown in circle B of Fig. 1c and d. The broken parts of the lamella rejoined together with an increased annealing time, as shown by circle B. When the temperature is increased to 167 °C, some residues of the tangential and radial lamellae can still be observed, as shown in Fig. 1f.

The melting of lath-like lamellae developed at 146 °C is shown in Fig. 2. Lath-like lamellae with branches on both sides can be observed clearly in Fig. 2a. As the temperature is increased from 146 to 155 °C, part of the lamella begins to melt, and changes occur on its edges, as indicated by framed areas A, B, and C in Fig. 2b–d. Upon further increasing the temperature to 161 °C, more parts of the lamellae melt. During the melting process, some of the melted parts are recovered, as shown in the framed area A of Fig. 2b and c, clearly indicating the occurrence of recrystallization. As the temperature is increased above 165 °C, most parts of the lamellae are melted, and distinct morphological changes take place, as shown in Fig. 2d–f. But even after the temperature is increased to 168 °C, some residues of the lamellae still exist. It is suggested that these unmelted residues are more stable regions formed during the melting and recrystallization processes. Our observations on the melting of lath-like lamellae verify the results of the crosshatched one. Even if all lamellae are formed at the same temperature, they have different thermal stability. Furthermore, the stability in different parts of one particular lamella is quite different. During the heating process, melting is always accompanied by perfection through recrystallization or reorganization.

Figure 3 shows the melting behaviors of edge-on (crosshatched) lamellae formed at 162 °C. We found no lamellar branches or tangential lamellae present at such a high crystallization temperature. As the temperature is increased from 162 to 169 °C, lamella 1 shrinks from its growth tip, as shown in Fig. 3a and b. Upon further increasing the temperature to 172 °C, obvious melting takes place in the lower part, and some of the edge-on lamellae in Fig. 3c are melted into segments, as shown in the framed areas of Fig. 3b–d. As the temperature is increased to 174 °C, some of the lamellar segments totally disappear, as shown in the framed area of Fig. 3d. As the temperature is increased from 174 to 175 °C, the edge-on lamellae are gradually melted from their growth tips to their center parts, as shown by the arrows in Fig. 3d–f. It seems that recrystallization or reorganization can still take place at

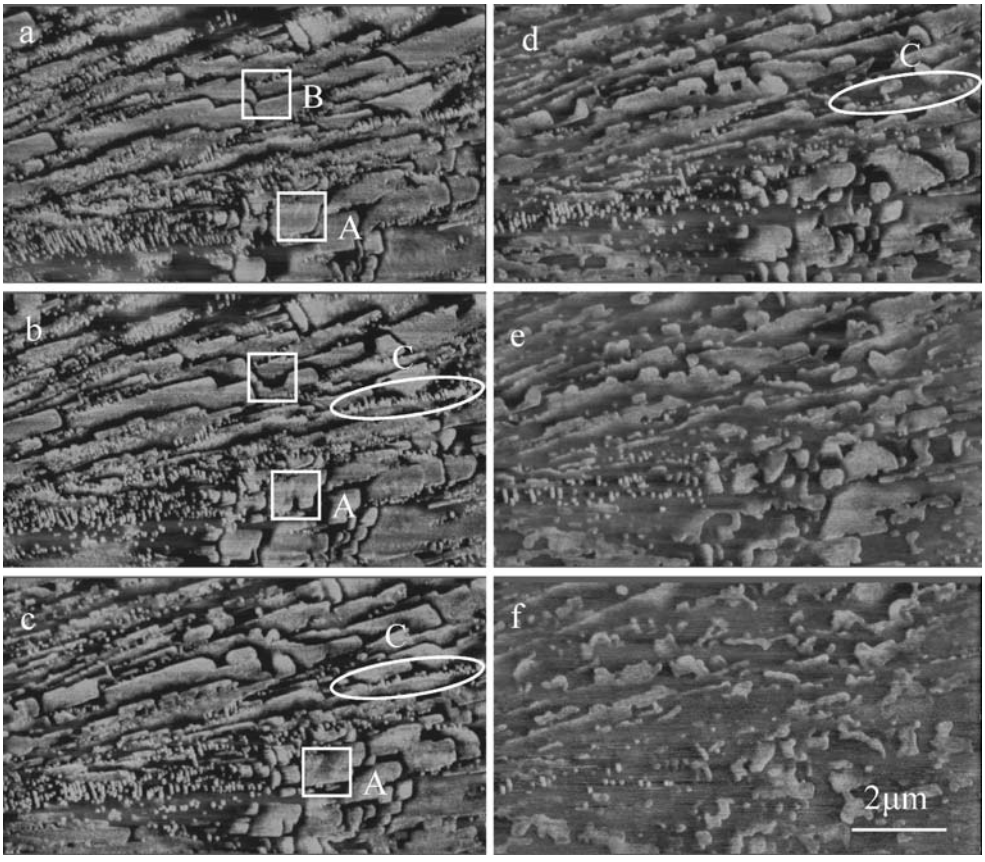


**Fig. 2** Melting of lath-like lamellae formed at 146 °C for about 60 min; **a** 146 °C, **b** 155 °C, **c** 161 °C, **d** 165 °C, **e** 167 °C, and **f** 168 °C. The time interval between two consecutive images is about 30 min

such high temperatures. After perfection, the lamellae tend to melt from their tips and gradually retract to their center parts. A similar melting behavior can be found on lath-like α-form lamellae formed at 162 °C, as shown in Fig. 4.

*Melting behavior of β-form lamellae* The α and β spherulites show quite different melting behaviors when heated to their melting temperatures. For samples containing both α and β spherulites, different crystalline form can be easily discriminated during DSC scan. The β-phase has a relatively lower melting point and melts first at about 152 °C, whereas the α-phase has a melting point of about 10 °C higher at about 164 °C. To compare the different melting behaviors of α and β lamellae, an interface between α and β spherulites is selected for AFM observation, as shown in Fig. 5. The extended sheet-like lamellae on the left and the densely crosshatched lamellae on the right are attributed to the β- and α-form lamellae, respectively, and both kinds of lamellar structures are developed at 146 °C. As the temperature increased from 146 to 154 °C, the β-form lamellae melt from the rim and gradually shrink to the center part, as shown by the arrow in Fig. 5b and c. At 154 °C (Fig. 5c), almost all the β-form lamellae are melted. Further increasing the temperature to 155 °C leads to the total disappearance of the β-form lamellae, whereas no significant morphological changes are found on the α-form lamellae, as shown in Fig. 5d. The radial direction of the crosshatched lamellae is indicated by an arrow in Fig. 5d. As the temperature is further increased from 155 to 168 °C, most of the crosshatched lamellae melt and both the radial and tangential lamellae disappear at the same time. The α-form lamellae formed at 146 °C melt completely when the temperature is increased to 169 °C (Fig. 5f). The newly formed α-form lamellae that crystallized in the melts of the β-form lamellae during the heating from 146 to 155 °C, which are more stable than those formed at 146 °C, cannot be melted at 169 °C (Fig. 5f). The detailed growth process of the α-form lamellae in the melts of the β-form lamellae can be found in our previous paper [30].

Our in situ AFM observations of α-form lamellae formed at 146 and 162 °C clearly show that increasing the crystallization temperature can shift the lamellar melting temperature up a great deal. Moreover, variation in crystallization temperatures leads to quite different lamellar structures and melting behaviors. The difference in melting behaviors can be attributed to the difference of the defect densities in the lamellae. It is commonly accepted that the lamellae crystallized at temperatures below the equilibrium melting point are always in a metastable state [31, 32]. The level of metastability is related to the degree of under-

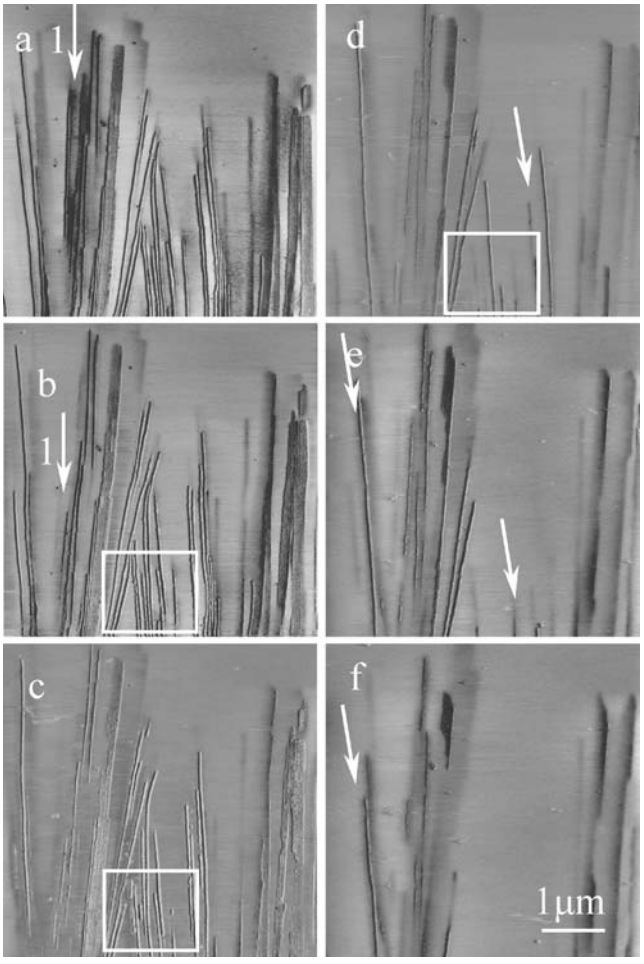


**Fig. 3** Melting of crosshatched lamellae formed at 162 °C for about 500 min; **a** 162 °C, **b** 169 °C, **c** 172 °C, **d** 174 °C, **e** 175 °C, and **f** 176 °C. The time interval between two consecutive images is about 30 min

cooling ($\Delta T$, the gap between crystallization temperature and equilibrium melting point), which is one of the main driving forces of crystallization. When crystallized at high undercooling, the chain diffusion is not as high, and packing of chains is not as perfect as for low undercooling. At high undercoolings, defects, such as chain ends, loops, stereoirregular sequences, etc., are more readily incorporated into the unit cell, resulting in local inhomogeneity within lamellae. As the temperature is increased, melting tends to start from these defective points, leading to partial melting of lamellae. At the same time, the molten parts can also adjust their chain conformation and repack into the lattice, resulting in recrystallization. So, both melting and recrystallization can be found in lamellae formed at high undercooling. For lamellae formed at low undercooling, such as 162 °C, the chains have more time to diffuse, adjust, and pack. The defect densities in lamellae should be much lower, so that melting starts at higher temperature, and reorganization or recrystallization is more difficult. But even for lamellae formed at such a high temperature, the lamellae are far from total perfection, and reorganization or recrystallization can still occur during the melting process. Some studies [12–15] have verified that reorganization or recrystallization takes place during high-temperature annealing, promoting transformation of the $\alpha$-phase from the less stable $\alpha$1-phase with a random distribution of up and down chain packing to the more stable $\alpha$2-phase with a well-defined deposition of up and down helices in the unit cell.

In our study of the lamellar growth at high temperatures [29], we have found that both the mother lamellae and the lamellar branches are formed at the same temperature, although the lamellar branches develop some distance behind the growth tip of the mother lamellae. Figures 1

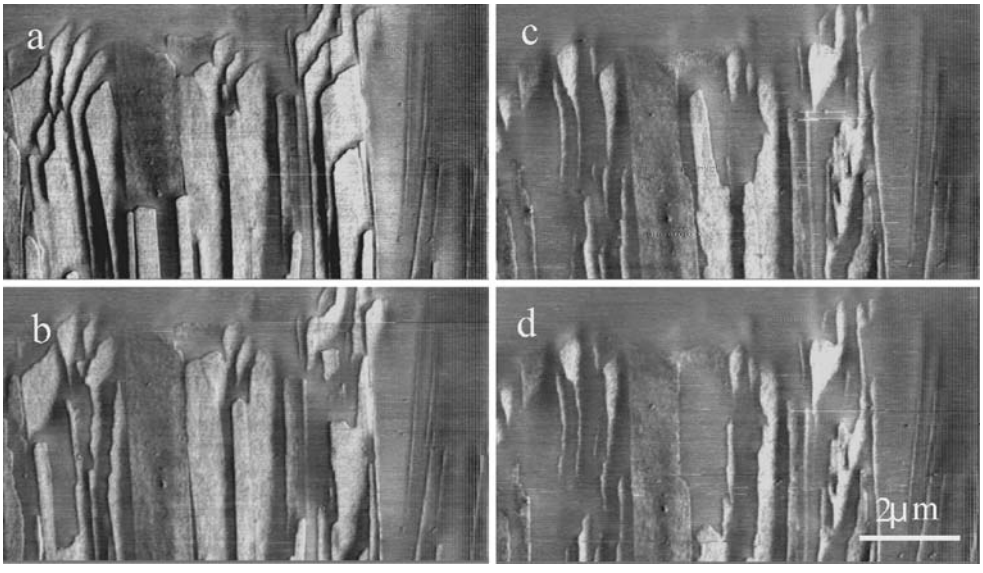


**Fig. 4** Melting of lath-like flamellae formed at 162 °C for about 500 min; **a** 162 °C, **b** 172 °C, **c** 175 °C, and **d** 177 °C. The time interval between two consecutive images is about 30 min

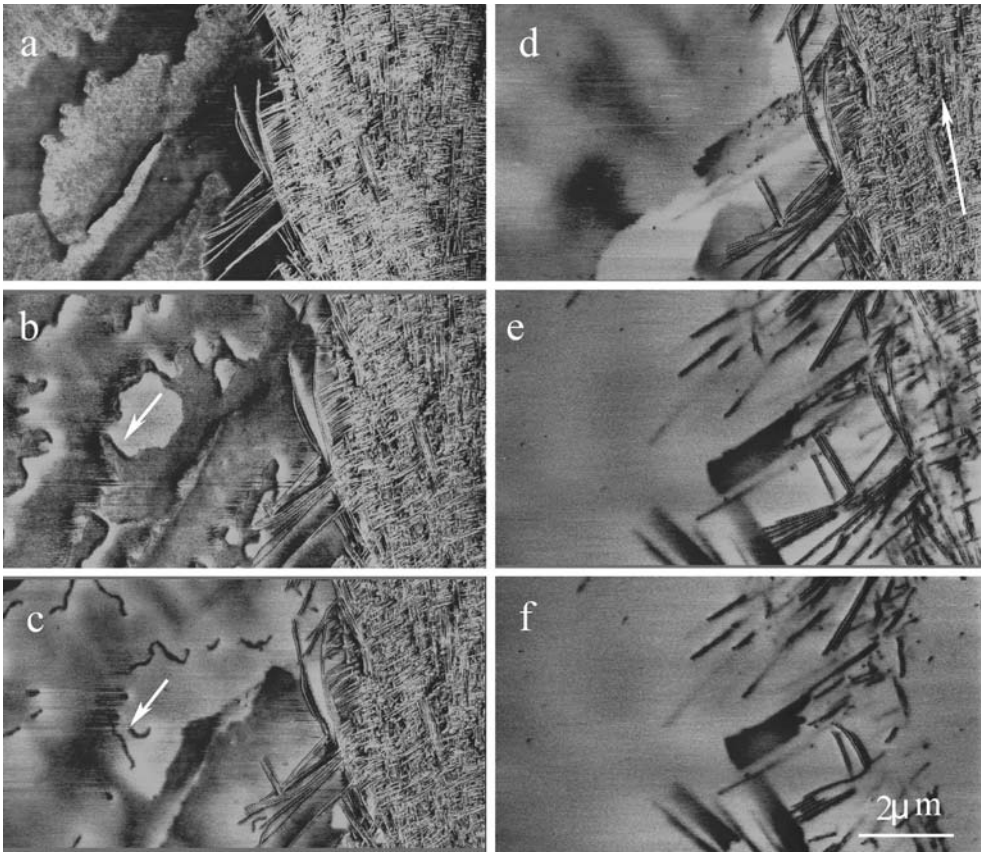


**Fig. 5** Melting of an interface between the α and β spherulites formed at 146 °C; **a** 146 °C, **b** 152°C, **c** 154 °C, **d** 155 °C, **e** 168 °C, and **f** 169 °C. The time interval between two consecutive images is about 30 min

and 2 show that these two kinds of lamellae also disappear at almost the same time, which strongly suggests that the multiple endothermal peaks, often observed during the heating scan of DSC measurements, cannot be simply attributed to the separate melting of these two kinds of lamellae. The lamellae melt in a wide range of temperatures, and melting starts from the defected parts. Moreover, recrystallization and reorganization can also take place during high-temperature annealing, including during a DSC heating run, leading to the melting of these recrystallized lamellar structures at higher temperatures.

## Conclusion

Using a hot-stage AFM, we followed the melting behaviors of α- and β-form *i*-PP lamellae in situ and in real time. The melting behavior of α-form lamellae is determined by the defects inside the lamellae. The more defects in the lamellae, the more easily the melting and recrystallization take place. Moreover, even for lamellae formed at very low undercoolings, the lamellae are far from being perfect, and recrystallization or reorganization can still take place at a higher temperature. Since both mother lamellae and lamellar branches disappear at almost the same temperature, it suggests that the origin of double endothermal peaks during DSC heating scan cannot be simply attributed to the special crosshatched structure of the mother and daughter lamellae. The α- and β-form lamellae melt separately, and the β-form lamellae melt first than the α-form lamellae.

**Acknowledgments** This work is supported by the Outstanding Youth Fund and the National Science Foundation of China (grant nos. 20325414, 20574083, and 50521302). We also thank Professor Jerold M. Schultz for his constructive comments.

## References

1. Keith HD, Padden FJ, Walter NM, Wyckoff HW (1959) J Appl Phys 30:1485
2. Al-Raheil IA, Qudah AM, Al-Share M (1998) J Appl Polym Sci 67:1267
3. Mezghani K, Campbell RA, Phillips PJ (1994) Macromolecules 27:997
4. Yadav YS, Jain PC (1986) Polymer 27:721
5. Janimak JJ, Cheng SZD, Zhang AQ (1992) Polymer 33:728
6. Samules RJ (1975) J Appl Polym Sci 13:1417
7. Zhang FJ, Gong YM, He TB (2003) Eur Polym J 39:2315
8. Weng J, Olley RH, Bassett DC, Jääskeläinen P (2002) J Macromol Sci Phys 41:891
9. Weng J, Olley RH, Bassett DC, Jääskeläinen P (2003) J Polym Sci Polym Phys 41:2342

10. Petraccone V, Guerra G, De Rosa C, Tuzi A (1985) Macromolecules 18:813
11. Paukkeri R, Lehtinen A (1993) Polymer 34:4083
12. De Rosa C, Guerra G, Napolitano R, Petraccone V, Pirozzi B (1984) Eur Polym J 20:937
13. Guerra G, Petraccone V, Corradini P, De Rosa C, Napolitano R, Pirozzi B (1984) J Polym Sci Polym Phys 22:1029
14. Corradi P, Napolitano R, Oliva L, Petraccone V (1982) Makromol Chem Rapid Commun 3:753
15. Naiki M, Kikkawa T, Endo Y, Nozaki K, Yamamoto T, Hara T (2000) Polymer 42:5471
16. Passingham C, Hendra PJ, Cudby MEA, Zichy V, Weller M (1990) Eur Polym J 26:631
17. Norton DR, Keller A (1985) Polymer 26:704
18. Dragaun H, Hubeny H, Muschik H (1977) J Polym Sci Polym Phys Ed 15:1779
19. Lovinger AJ, Chua JD, Gryte LC (1977) J Polym Sci Polym Phys Ed 15:641
20. Turner-Jones A, Cobbold AJ (1968) J Polym Sci 6:539
21. Varga J (1992) J Mater Sci 27:2557
22. Matheu C, Thierry JC, Wittmann JC, Lotz B (2002) J Polym Sci Polym Phys 40:2504
23. Varga J (1986) J Therm Anal 31:165
24. Varga J (1992) J Mater Sci 27:2557
25. Godovsky YK, Magonov SN (2000) Langmuir 16:3549
26. Winkel AK, Hobbs JK, Miles MJ (2000) Polymer 41:8791
27. Zhou W, Cheng SZD, Putthanarat S, Eby RK, Reneker DH, Lotz B, Magonov S, Hsieh ET, Geerts RG, Palackal SJ, Hawley GR, Welch M (2000) Macromolecules 33:6861
28. Jiang Y, Jin XG, Han CC, Li L, Wang Y, Chan CM (2003) Langmuir 19:8010
29. Zhou JJ, Liu JG, Yan SK, Dong JY, Li L, Chan CM, Schultz JM (2005) Polymer 46:4077
30. Zhou JJ, Li L, Lu J (2006) Polymer 47:261–264
31. Keller A, Cheng SZD (1998) Polymer 39:4461
32. Cheng SZD, Keller A (1998) Annu Rev Mater Sci 28:533